

# Kinetics of the $R + HBr \rightarrow RH + Br$ ( $R = CH_2I$ or $CH_3$ ) reaction. An *ab initio* study of the enthalpy of formation of the $CH_2I$ , $CHI_2$ and $CI_3$ radicals

Jorma A. Seetula

Laboratory of Physical Chemistry, P.O. Box 55 (A.I. Virtasen aukio 1), FIN-00014 University of Helsinki, Helsinki, Finland

Received 15th August 2001, Accepted 7th November 2001

First published as an Advance Article on the web 15th January 2002

The kinetics of the reaction of the  $CH_2I$  and  $CH_3$  radicals,  $R$ , with  $HBr$  have been investigated separately in a heatable tubular reactor coupled to a photoionization mass spectrometer. The  $CH_2I$  (or  $CH_3$ ) radical was produced homogeneously in the reactor by a pulsed 248 or 351 nm exciplex laser photolysis of  $CH_2I_2$  (or  $CH_3I$ ). The decay of  $R$  was monitored as a function of  $HBr$  concentration under pseudo-first-order conditions to determine the rate constants as a function of temperature. The reactions were studied separately over a wide ranges of temperatures and the rate constants determined were fitted to an Arrhenius expression (error limits stated are  $1\sigma +$  Student's  $t$  values, units in  $cm^3 \text{ molecule}^{-1} \text{ s}^{-1}$ ):  $k(CH_2I + HBr) = (3.8 \pm 0.7) \times 10^{-13} \exp[+(1.4 \pm 0.6) \text{ kJ mol}^{-1}/RT]$  and  $k(CH_3 + HBr) = (2.3 \pm 0.5) \times 10^{-12} \exp[+(0.60 \pm 0.17) \text{ kJ mol}^{-1}/RT]$ . The threshold energies of the reverse reactions,  $Br + R'H \rightarrow R' + HBr$  ( $R' = CH_2I$ ,  $CHI_2$  or  $CI_3$ ), were calculated by *ab initio* methods at the MP2(fc)/6-311G(df)//MP2(fc)/6-311G(df) level of theory. These were combined with the experimentally determined activation energies of the forward reactions in a second-law method to determine the enthalpies of the reactions. The enthalpy of formation values at 298 K are (in  $\text{kJ mol}^{-1}$ ):  $228.0 \pm 2.8$  ( $CH_2I$ ),  $314.4 \pm 3.3$  ( $CHI_2$ ) and  $424.9 \pm 2.8$  ( $CI_3$ ). The C–H bond strengths of analogous iodomethanes are (in  $\text{kJ mol}^{-1}$ ):  $431.6 \pm 2.8$  ( $CH_3I$ ),  $412.9 \pm 3.3$  ( $CH_2I_2$ ) and  $391.9 \pm 3.1$  ( $CHI_3$ ). The Arrhenius expression of the reverse reactions as determined by the thermodynamic transition state theory. The entropies of activation of the reactions were obtained by *ab initio* calculations.

## Introduction

Iodomethane is largely used as a methylation agent in organic chemistry. Its natural source has been identified as pelagic ocean and ocean surface waters and recently volcanic production.<sup>1,2</sup> The natural source of diiodomethane has been found to be a marine phytoplankton.<sup>3</sup>

The current study presents a time-resolved experimental kinetic investigation of the  $CH_2I$  and the  $CH_3$  radicals with  $HBr$ . The first reaction has not previously been studied. The approach is similar to that used for the study of chlorinated radicals with  $HBr$ .<sup>4</sup> The current study was carried out to investigate the enthalpy of formation of the  $CH_2I$  using a second-law method. For this, *ab initio* calculations were needed to study the different reaction channels of the  $Br + CH_3I$  reaction. Of these, the H atom abstraction reaction cannot be studied experimentally, as the I atom abstraction reaction is the dominant channel. The quantum chemical calculations were further used in conjunction with a second-law method to extend the kinetic and thermodynamic studies to include  $CHI_2$  and  $CI_3$  free radical reactions with  $HBr$  in order to obtain the other C–H bond energies of iodinated methanes for comparison. It was shown previously that Cl atoms significantly decrease the  $C_\alpha$ -H bond strength of alkyl chlorides by decreasing the threshold barrier of the H atom abstraction reaction.<sup>5</sup> A similar effect can be expected to occur with I atoms.

## Kinetics and computational

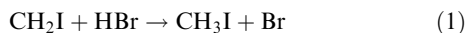
### Description of kinetic experiments

The rate constants of the reaction of  $CH_2I$  or  $CH_3$  with  $HBr$  were measured as a function of temperature. The experimental apparatus used has been described previously.<sup>6,7</sup> Pulsed, unfocused 351 or 248 nm radiation from a Lambda Physik EMG 201 MSC exciplex laser operated at 5 Hz was collimated and then directed along the axis of a heatable Pyrex reactor. The 10.5 mm id reactor was coated with fluorinated halo-carbon wax or Teflon to reduce heterogeneous reactions. Gas flowing through the tube at  $5 \text{ m s}^{-1}$  was completely replaced between laser pulses. The flowing gas contained the radical precursor  $CH_2I_2$  ( $< 0.1\%$ ),  $HBr$  in varying concentrations and the carrier gas, He, in large excess ( $> 98\%$ ). Gas was sampled through a 0.44 mm id hole located at the end of a nozzle in the wall of the reactor and was formed into a beam by a conical skimmer before it entered the vacuum chamber containing the quadrupole mass filter. As the gas beam traversed the ion source, a portion was photoionized by VUV light and then mass selected. Temporal ion signal profiles were recorded, from 10–30 ms before each laser pulse and 16–25 ms after the laser pulse, with a multichannel scalar. Data from 1000 to 11000 repetitions of the experiments were accumulated for analysis by a non-linear least-squares analysis program.

At the photolysis wavelengths used to generate  $\text{CH}_3$  or  $\text{CH}_2\text{I}$  radicals, it is practically impossible to photodissociate the reactant,  $\text{HBr}$ , to a measurable extent.<sup>8</sup>

### Kinetic results from experimental studies

The chemical kinetics of the following metathetical reactions were studied separately:



The temperature dependence determined for reaction (1) was combined with the quantum chemically calculated threshold energy of the reverse reaction, (-1), in order to calculate the enthalpy of formation of the  $\text{CH}_2\text{I}$  radical. The results obtained from the experiments to measure reactions (1) and (2) are given in Table 1. Reaction (2) was remeasured to calibrate the experimental conditions used by comparing the kinetic data obtained with the previously measured rate constants of the same reaction.

### Photogeneration of $\text{CH}_2\text{I}$ and $\text{CH}_3$ radicals

The  $\text{CH}_2\text{I}$  radical was photogenerated by photodissociating  $\text{CH}_2\text{I}_2$  at 248 or 351 nm. Up to 9 meshes or a thick vycor plate were used to diminish laser fluence to a very low level. This ensured that the photon flux did not generate  $\text{Br}$  atoms from  $\text{HBr}$  to any measurable extent or that any  $\text{CH}_2\text{I}$  radical recombination reaction was too slow to interfere with the kinetics observed because the initial  $\text{CH}_2\text{I}$  radical concentration was below  $10^{11}$  radical  $\text{cm}^{-3}$ . The  $\text{CH}_2\text{I}$  radical was formed from the precursor by C–I bond rupture. The main photodissociation process is to generate  $\text{CH}_2\text{I} + \text{I}(^2\text{P}_{1/2}$  or  $^2\text{P}_{3/2})$  at 248 and 351 nm.<sup>9</sup> The quantum yield of  $\text{I}(^2\text{P}_{1/2})$  is 0.46 at 248 nm and decreases to nonexistence at 355 nm.<sup>9,10</sup>

**Table 1** Measurements of the rate constant of the  $\text{R} + \text{HBr} \rightarrow \text{Br} + \text{RH}$  ( $\text{R} = \text{CH}_2\text{I}$  or  $\text{CH}_3$ ) reaction

$T^a/\text{K}$	$[\text{He}]/10^{16} \text{ cm}^{-3}$	$[\text{HBr}]/10^{13} \text{ cm}^{-3}$	$k_3/\text{s}^{-1}$	$k_1^b/10^{-13} \text{ cm}^3 \text{ s}^{-1}$
<b><math>\text{CH}_2\text{I} + \text{HBr} \rightarrow \text{Br} + \text{CH}_3\text{I}</math> (<math>k_1</math>)</b>				
297	2.83	8.74–39.2	16	$6.5 \pm 0.4^c$
298	5.79	5.70–34.7	19	$6.6 \pm 0.6^c$
299	5.81	9.66–47.5	25	$6.9 \pm 0.7^d$
328	5.81	11.6–46.5	15	$6.0 \pm 0.5^c$
363	5.83	11.1–53.1	15	$6.2 \pm 0.4^c$
408	5.84	11.8–43.7	15	$5.7 \pm 0.4^d$
465	5.85	9.31–58.2	18	$5.3 \pm 0.4^d$
$k_1 = (3.8 \pm 0.7) \times 10^{-13} \exp[(1.4 \pm 0.6) \text{ kJ mol}^{-1}/RT] \text{ cm}^3 \text{ molecule}^{-1} \text{ s}^{-1}$				
<b><math>\text{CH}_3 + \text{HBr} \rightarrow \text{Br} + \text{CH}_4</math> (<math>k_2</math>)</b>				
299	5.82	2.32–11.4	8.7	$29.3 \pm 2.1^d$
300	17.8	3.05–8.54	15	$29.2 \pm 0.9^d$
348	5.89	5.83–11.1	9.5	$29.3 \pm 0.5^d$
348	5.89	2.07–7.21	7.2	$31.5 \pm 1.2^d$
409	5.85	3.28–8.59	13	$25.9 \pm 0.8^d$
510	5.86	2.02–6.58	17	$25.3 \pm 1.0^d$
510	5.87	2.14–8.70	1.5	$26.0 \pm 1.0^d$
677	5.88	1.91–9.80	5.7	$27.4 \pm 0.8^d$
$k_2 = (2.3 \pm 0.5) \times 10^{-12} \exp[(0.60 \pm 0.17) \text{ kJ mol}^{-1}/RT] \text{ cm}^3 \text{ molecule}^{-1} \text{ s}^{-1}$				

<sup>a</sup> Temperature uncertainty:  $\pm 1$  for 299–328 K and  $\pm 3$  for 348–677 K. <sup>b</sup> Fluorinated halocarbon wax used for wall coating at 297–363 K, Teflon at 408–510 K and  $\text{B}_2\text{O}_3$  at 510–677 K, errors are  $1\sigma$  + Student's  $t$  and are based on statistical uncertainties. <sup>c</sup> 351 nm photolysis. <sup>d</sup> 248 nm photolysis.

Moreover, collisional deactivation of the vibrationally excited  $\text{CH}_2\text{I}$  radical occurs rapidly ( $< 0.5$  ms) compared to the time-scale used.<sup>9</sup> The formation of  $\text{CH}_2 + \text{I}_2$ , is energetically possible at 248 nm but forbidden by symmetry considerations. Also the products of this channel were not detected in the current study.

The  $\text{CH}_3$  radical was generated by photolysis of  $\text{CH}_3\text{I}$  at 248 nm. The main photolysis channel is the formation of  $\text{CH}_3 + \text{I}(^2\text{P}_{1/2})$ .<sup>9</sup>

The absorption spectrum of  $\text{CH}_2\text{I}_2(\text{g})$  at 308 K is shown as an insert of Fig. 1. The wavelengths of both laser lines used are shown in the insert to demonstrate that the photodissociation occurred *via* a different electronic excitation of the precursor, depending on the wavelength used. The spectrum was recorded using a dual beam Cary 100 spectrophotometer. The resolution used was 0.2 nm. The quartz absorption cell of 5 cm length used with a thermostatable cell holder was coupled to a thermostating bath to maintain a constant temperature in the cell.

### Data analysis

Experiments were conducted under pseudo-first-order conditions where  $\text{HBr}$  existed in great excess compared with the concentration of radicals. Only the following two reactions had significant rates under these conditions:



In all sets of experiments the initial radical concentration was adjusted to be so low that radical–radical or radical–atom reactions had negligible rates compared to reactions (1)–(3). This was ensured by comparing the measured first-order wall loss decays,  $k_3$ , of the radical with that produced (in the absence of  $\text{HBr}$ ) at different conditions where precursor

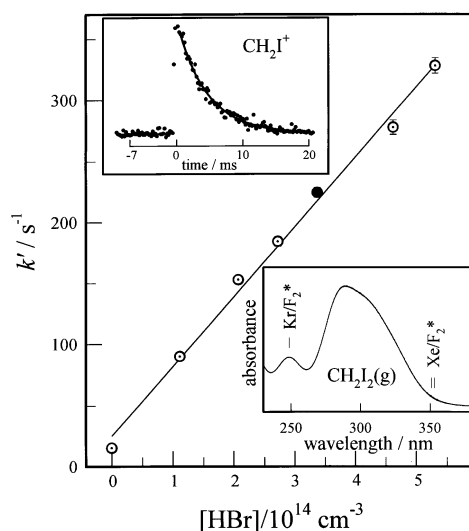


**Fig. 1** Plot of first-order decay constant  $k'$  vs.  $[\text{HBr}]$  for one set of experiments conducted to measure the  $\text{CH}_2\text{I} + \text{HBr}$  rate constant,  $k_1$ , at 363 K. The insert in the upper left corner is the ion signal profile of  $\text{CH}_2\text{I}^+$  recorded during one of the experiments shown as a solid circle ( $[\text{HBr}] = 3.37 \times 10^{14} \text{ molecule cm}^{-3}$ ) in the linear regression fit. The line through the data in the insert is an exponential function fitted by a nonlinear least-squares procedure. The first-order decay constant for  $\text{CH}_2\text{I}^+$  in the displayed ion signal profile is  $(224.7 \pm 3.9) \text{ s}^{-1}$ . The insert in the lower right corner is the gas phase absorption spectrum of  $\text{CH}_2\text{I}_2$  at 308 K. The resolution of the spectrum is 0.2 nm. The two maxima shown are at 248.4 nm and 288.4 nm. The  $\text{CH}_2\text{I}$  radical was photogenerated from  $\text{CH}_2\text{I}_2$  by a  $\text{Xe}/\text{F}_2^*$  emission wavelength of the exciplex laser to study the data set shown.

concentration was held steady but the laser radiation was attenuated by the use of 2 meshes and a Vycor plate (the radical concentration was changed by the same factor). The decays from these different experiments were equal with respect to their statistical error limits.

Rate constants for reactions (1) and (2) were obtained from the slopes of plots of the exponential radical decay constant  $k'$  vs.  $[\text{HBr}]$  {from  $[\text{R}^+]_t = [\text{R}^+]_0 \exp(-k't)$ }, where  $k' = k_{1 \text{ or } 2} [\text{HBr}] + k_3$ . A representative ion signal decay profile and a decay constant plot from one set of experiments to measure  $k_1$  are shown in Fig. 1. The results obtained from all the experiments to measure reactions (1)–(3) are given in Table 1.

### Accuracy of measurements

The error limits stated in the Arrhenius expressions are  $1\sigma + \text{Student's } t$  and they are based only on the statistical uncertainties. The reactions were studied under pseudo-first-order conditions when it was needed to know accurately only the concentration of HBr. The other errors, such as measured temperature and gas flow rates, were always  $< 1\%$ . All these errors are very small and were thus ignored. The statistical uncertainties of the decay constants were taken into account in data analysis and their effects on the rate constants are shown in Fig. 2. The Arrhenius expression of the reaction was obtained by weighting the measured rate constants with reciprocals of their variances for the fitting procedure.

### Reagent sources and purification procedures

$\text{CH}_2\text{I}_2$ , 99%,  $\text{CH}_3\text{I}$ , 99.5%, and HBr, 99%, were obtained from Aldrich and helium, 99.995%, from Matheson.

The carrier gas, He, was used as provided.  $\text{CH}_2\text{I}_2$  and  $\text{CH}_3\text{I}$  were degassed by using freeze–pump–thaw cycles, stabilized with copper and stored in darkness. The vaporized precursor gas was mixed with the carrier gas flow before it entered the reactor inlet. HBr was collected to a flow trap kept at 77 K and was repeatedly distilled to remove any traces of bromine. HBr was stored in a dark Pyrex bulb. The flow of precursor/He mixture and HBr were not mixed until they reached the reactor. The gas handling system, which was used to set up a known HBr flow to the reactor gas inlet, was made from Pyrex glass and Teflon tubes.

### Photoionization energies used

Reactants and products of the photolysis as well as the precursors were photoionized using atomic resonance radiation. A chlorine lamp (8.9–9.1 eV) coupled with a  $\text{CaF}_2$  salt window was used to detect  $\text{CH}_2\text{I}$ , a hydrogen lamp (10.2 eV; with a

$\text{MgF}_2$  window) to detect  $\text{CH}_3$ , I,  $\text{CH}_3\text{I}$  and  $\text{I}_2$  and an argon lamp (11.6, 11.8 eV; with a LiF window) to detect HBr,  $\text{Br}_2$  and Br.

### Computation details

*Ab initio* calculations were carried out with the Gaussian 98 package of programs.<sup>11</sup> All calculations were carried out on an Origin 2000 computer at the Centre for Scientific Computing (Espoo, Finland). All structures of species needed for the transition state calculations were fully optimized at the MP2 level of theory using 6-311G basis set with supplementary functions for d and f shells [labelled as 6-311G(df)], and frozen-core approximation.<sup>12</sup> The basis sets for I and Br are taken from the literature.<sup>13,14</sup> The transition state of the equilibrium reaction was localized at the minimum energy path using a quadratic synchronous transit method.<sup>12</sup> In the calculations the expectation values,  $S^2$ , for free radicals were in the range 0.7579–0.7918 and for transition states in the range 0.7920–0.8062. Normal mode analyses were carried out at the same level of theory for all species and transition states. These frequency calculations show the optimized transition state to be a first-order saddle point with all the second derivatives of energy being positive except for one, which has an imaginary vibrational frequency along the reaction coordinate. The imaginary frequencies were in the range  $-746 \text{ cm}^{-1}$  to  $-1180 \text{ cm}^{-1}$ . The internal coordinates of the transition state, which according to the calculated normal modes experience the largest changes during the reaction, are the C–H and H–Br bond lengths. The relative movement of the H atom is the largest. The C–H–Br asymmetric stretch is the reaction coordinate. Unscaled harmonic frequencies were used in the calculations. Zero-point energy corrected energies of the reactants of the reverse reactions were compared to that of the reaction transition state for the threshold energy calculation at 0 K (see Table 2). The *ab initio* calculations were needed to determine the kinetics of the Br + molecule reactions.

### Computationally calculated kinetics of the reverse reactions

*Ab initio* calculations were also used to determine the entropies of the reactants and the transition states of  $\text{Br} + \text{RH} \rightarrow \text{HBr} + \text{R}$  ( $\text{R} = \text{CH}_2\text{I}$ ,  $\text{CHI}_2$  or  $\text{Cl}_3$ ) reactions (see Tables 3 and 4 for structural parameters, frequencies and moments of inertia). The Arrhenius expressions of the bimolecular reactions at 298.15 K were obtained using thermodynamic transition state theory.

The canonical rate constant used is

$$k(T) = \frac{\kappa L^\ddagger e^2 k_B T}{hc^0} \exp\left(\frac{\Delta_r S^\ddagger - 371.26}{R}\right) \exp\left(-\frac{E_a}{RT}\right)$$

where  $\kappa$  = transmission coefficient,<sup>15</sup>  $L^\ddagger$  = reaction path degeneracy,  $k_B$  = Boltzmann constant,  $h$  = Planck's constant,

**Table 2** Symmetry point groups, total and zero-point energies. Energies at the MP2(fc)/6-311G(df)//MP2(fc)/6-311G(df) level are in  $E_h$

Compound	Symmetry	Total energy	Zero-point energy
Br	$K_h$	-2572.639864	0.0
HBr	$C_{\infty v}$	-2573.271159	0.006172
$\text{CH}_3\text{I}$	$C_{3v}$	-6956.834592	0.037418
$\text{CH}_2\text{I}$	$C_s$	-6956.174294	0.022203
$\text{CH}_2\text{I}_2$	$C_{2v}$	-13873.317448	0.027787
$\text{CHI}_2$	$C_s$	-13872.664184	0.014140
$\text{CHI}_3$	$C_{3v}$	-20789.798621	0.017211
$\text{Cl}_3$	$C_{3v}$	-20789.153875	0.004797
$\text{Br-H-CH}_2\text{I}$	$C_1$	-9529.443493	0.030083
$\text{Br-H-CHI}_2$	$C_1$	-16445.932381	0.020610
$\text{Br-H-Cl}_3$	$C_1$	-23362.419833	0.010161

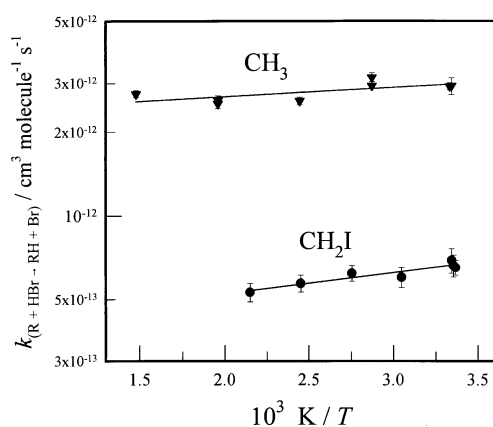


**Fig. 2** Arrhenius plot of  $\text{CH}_2\text{I} + \text{HBr}$  and  $\text{CH}_3 + \text{HBr}$  reactions measured in the current study. The lines are Arrhenius expressions fitted to the rate constants  $k_1$  and  $k_2$ .

**Table 3** Structural parameters of the species optimized in *ab initio* calculations at the MP2(fc)/6-311G(df)//MP2(fc)/6-311G(df) level of theory. Bond lengths in Å and angles in degrees<sup>a</sup>

Species	$r_{\text{CH}}$	$r_{\text{CI}}$	$r_{\text{C-H}}$	$r_{\text{H-Br}}$	$a_{\text{ICH}}$	$a_{\text{HCH}}$	$a_{\text{ICI}}$	$a_{\text{d}}$	$a_{\text{C-H-Br}}$	$a_{\text{o}}$
CH <sub>3</sub> I	1.087	2.137	—	—	108.1	110.8	—	—	—	—
CH <sub>2</sub> I	1.079	2.044	—	—	118.5	122.4	—	—	—	8.5
CH <sub>2</sub> I <sub>2</sub>	1.086	2.135	—	—	107.7	111.3	114.8	—	—	—
CHI <sub>2</sub>	1.083	2.052	—	—	116.7	—	122.6	—	—	23.3
CHI <sub>3</sub>	1.087	2.143	—	—	106.4	—	112.4	—	—	—
Cl <sub>3</sub>	—	2.068	—	—	—	—	118.8	—	—	19.3
Br-H-CH <sub>2</sub> I	1.085	2.061	1.523	1.529	114.9	117.2	—	180	170.4	36.5
Br-H-CHI <sub>2</sub>	1.088	2.078	1.467	1.549	112.6	—	119.5	180	185.1	40.5
Br-H-Cl <sub>3</sub>	—	2.104	1.403	1.580	—	—	115.0	180	180	38.0

<sup>a</sup> The bond length of HBr is 1.416 Å. The dihedral angle  $a_{\text{d}}$  is given as  $a_{3126}$  (see Fig. 3) and the out-of-plane angle  $a_{\text{o}}$  at the radical center of the transition state or free radical is an angle between a plane (consists of a C and two H or I) and a remaining bond.

**Table 4** Moments of inertia and unscaled vibrational frequencies as wavenumbers of the species calculated at the MP2(fc)/6-311G(df)//MP2(fc)/6-311G(df) level of theory. The numbers in parentheses refer to two similar wavenumbers if given as integers

Compound	Wavenumber/cm <sup>-1</sup>	Moment of inertia/10 <sup>-47</sup> kg m <sup>2</sup>
CH <sub>2</sub> I	170, 659, 898, 1421, 3222, 3376	3.011, 94.95, 97.93
CH <sub>3</sub> I	574, 933(2), 1343, 1513(2), 3125, 3246(2)	5.365, 111.8, 111.8
Br-H-CH <sub>2</sub> I	60, 305, 436, 670, 834, 886, 951, 1171, 1419, 3171, 3302, 746i	49.47, 1478, 1522
CHI <sub>2</sub>	132, 326, 548, 760, 1189, 3253	25.12, 1368, 1393
CH <sub>2</sub> I <sub>2</sub>	121, 515, 630, 756, 1106, 1188, 1462, 3165, 3254	37.63, 1368, 1400
Br-H-CHI <sub>2</sub>	45, 91, 135, 324, 615, 687, 788, 944, 1056, 1164, 3197, 950i	1374, 1405, 2752
Cl <sub>3</sub>	112(2), 154, 219, 754(2)	1338, 1338, 2673
CHI <sub>3</sub>	105(2), 160, 453, 626(2), 1141(2), 3194	1349, 1349, 2675
Br-H-Cl <sub>3</sub>	48(2), 110(2), 123, 196, 669(2), 726, 880(2) 1180i	2635, 2635, 2659
HBr	2709	3.320

$T$  = absolute temperature,  $R$  = universal gas constant,  $\Delta_r S^{\ddagger}$  = standard entropy of activation of the reaction and  $E_{\text{a}}$  = Arrhenius activation energy. The  $\Delta_r S^{\ddagger} = S^{\ddagger} - \sum S^{\circ}$  (reactants) refers to a standard state of  $c^{\circ}$  (molecule cm<sup>-3</sup>). The value of 371.26 (in J K<sup>-1</sup> mol<sup>-1</sup>) changes the standard state from 1 atm to molecule cm<sup>-3</sup>.<sup>16</sup> Arrhenius activation energies at 298.15 K were calculated from the heat capacity corrected threshold energies. The Arrhenius rate expressions determined at 298.15 K are as follows:

$$k(\text{Br} + \text{CH}_3\text{I} \rightarrow \text{HBr} + \text{CH}_2\text{I}) = 3.3 \times 10^{-11} \times \exp(-63.9 \text{ kJ mol}^{-1}/RT) \text{ cm}^3 \text{ molecule}^{-1} \text{ s}^{-1}$$

$$k(\text{Br} + \text{CH}_2\text{I}_2 \rightarrow \text{HBr} + \text{CHI}_2) = 1.5 \times 10^{-11} \times \exp(-48.0 \text{ kJ mol}^{-1}/RT) \text{ cm}^3 \text{ molecule}^{-1} \text{ s}^{-1}$$

$$k(\text{Br} + \text{CHI}_3 \rightarrow \text{HBr} + \text{CI}_3) = 5.0 \times 10^{-12} \times \exp(-29.9 \text{ kJ mol}^{-1}/RT) \text{ cm}^3 \text{ molecule}^{-1} \text{ s}^{-1}$$

Error limits for the  $A$  factors are not considered, for the activation energies they are typically  $\pm 2.4$  kJ mol<sup>-1</sup> in comparison with experimentally determined activation energies with quantum chemically calculated threshold energies.<sup>5</sup> The effect of rotational symmetry of the molecule in its rotational entropy is included in the  $E^{\ddagger}$  and excluded from the value of  $\Delta_r S^{\ddagger}$ . Furthermore, the tunnelling effect is ignored because activation energies of the forward reactions are in the range (-0.2–4.3) kJ mol<sup>-1</sup> and either Wigner or unsymmetrical Eckart barrier correction overestimates the tunnelling effect for the reverse reactions. The calculated Arrhenius  $A$  factors per H atom are  $11.0 \times 10^{-12}$  and  $7.6 \times 10^{-12}$  and  $5.0 \times 10^{-12}$  cm<sup>3</sup> molecule<sup>-1</sup> s<sup>-1</sup>. The trend of decreasing  $A$  factors per H atom as a function of increasing iodination substitution on methane is similar to that of the reactions of Br atom with CH<sub>3</sub>Cl and CH<sub>2</sub>Cl<sub>2</sub>.<sup>4</sup>

## Thermochemical calculations

In the reactions of the  $\text{R} + \text{HBr} \rightleftharpoons \text{RH} + \text{Br}$  ( $\text{R} = \text{CH}_2\text{I}$ ,  $\text{CHI}_2$  or  $\text{Cl}_3$ ) equilibrium no mole change is involved. Consequently, the standard reaction enthalpy change,  $\Delta_r H^{\circ}$ , is simply the difference between the activation energies of the reaction directions. The kinetics of  $\text{CH}_2\text{I} + \text{HBr}$  reaction was determined experimentally whereas the temperature dependences of  $\text{CHI}_2/\text{Cl}_3 + \text{HBr}$  reactions were estimated using a linear

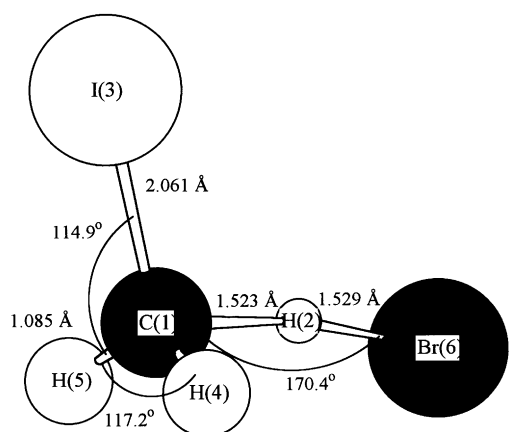


**Fig. 3** Optimized transition state of the  $\text{Br} + \text{CH}_3\text{I} \rightarrow \text{CH}_2\text{I} + \text{HBr}$  reaction at 0 K. The parameters are calculated at the MP2(fc)/6-311G(df)//MP2(fc)/6-311G(df) level of theory. The dihedral angle  $a_{\text{d}} = a_{3126} = 180^\circ$ .

**Table 5** Heats of formation used in the thermochemical calculations

Species	$\Delta_f H_{298}^0 / \text{kJ mol}^{-1}$
HBr <sup>a</sup>	$-36.44 \pm 0.17$
Br <sup>a</sup>	$111.86 \pm 0.06$
CH <sub>3</sub> I <sup>b</sup>	$14.4 \pm 1.4$
CH <sub>2</sub> I <sub>2</sub> <sup>b</sup>	$119.5 \pm 2.2$
CHI <sub>3</sub> <sup>b</sup>	$251.0 \pm 1.4$

<sup>a</sup> Data taken from ref. 18. <sup>b</sup> Data taken from ref. 19.

relationship between the experimental activation energies of free radical (R) reactions with HBr and the algebraic sum of Pauling's electronegativities of the atoms attached to the radical carbon in R.<sup>5,17</sup>

For a second-law calculation the mean temperature on a  $1/T$  scale of the studied reaction directions is always near 0 K if the other activation energy is determined at absolute zero of temperature. In the current study the threshold energies of Br + molecule reactions, which at 0 K exactly equals the activation energies, are calculated using the *ab initio* method. Furthermore, the enthalpies of the reactions near 0 K are corrected to 298 K using a heat capacity correction. For these calculations the heat capacity values at constant pressure of Br and HBr were taken from the literature. For the other compounds studied, the *ab initio* calculated heat capacity values at constant volume were used instead. However, for an ideal gas reaction with no mole change these two heat capacities are similar. The mean standard heat capacity of the reaction over the temperature range 0–298 K is about half of the value at 298 K.<sup>5</sup> Finally, the enthalpies of formation of the radicals studied were calculated using the enthalpies of reaction and the enthalpy of formation,  $\Delta_f H_{298}^0$ , values of Br, HBr and iodinated methane (see Table 5). The values obtained are as follows:

$$\Delta_f H_{298}^0(\text{CH}_2\text{I}) = 228.0 \pm 2.8 \text{ kJ mol}^{-1}$$

$$\Delta_f H_{298}^0(\text{CHI}_2) = 314.4 \pm 3.3 \text{ kJ mol}^{-1}$$

$$\Delta_f H_{298}^0(\text{CI}_3) = 424.9 \pm 2.8 \text{ kJ mol}^{-1}$$

The enthalpy of formation of CH<sub>2</sub>I can be obtained from the C–H bond energy of CH<sub>3</sub>I at 298 K to be a value of  $431.6 \pm 2.8 \text{ kJ mol}^{-1}$ . Similarly the other C–H bond energies obtained are  $412.9 \pm 3.3 \text{ kJ mol}^{-1}$  of CH<sub>2</sub>I<sub>2</sub> and  $391.9 \pm 3.1 \text{ kJ mol}^{-1}$  of CHI<sub>3</sub> at 298 K.

## Discussion

### Collisionally relaxed radicals

A great advantage of using 351 nm photolysis instead of 193 nm photolysis (commonly used to generate free radicals in the gas phase for kinetic purposes) is that one can generate the radical of interest with less excess internal energy. Furthermore, the vibrational deactivation of a small polyatomic free radical is very fast already at a few torr pressure. This phenomenon is concluded from the CH<sub>3</sub> + HBr studies of Krasnoperov *et al.* over the pressure range from 1 to 100 bar.<sup>20</sup> The authors used 193 nm photolysis of acetone to generate the CH<sub>3</sub> radical and studied the kinetics of this radical reaction by using time-resolved transient UV spectroscopy. A weighted rate constant value of  $(3.2 \pm 1.0) \times 10^{-12} \text{ cm}^3 \text{ molecule}^{-1} \text{ s}^{-1}$  can be calculated from the set of rate constants measured by the authors at  $297 \pm 3 \text{ K}$  over a wide pressure range. The closeness of the values of the rate constants implies that the CH<sub>3</sub> + HBr reaction has no pressure dependence. Here the rate constant

was remeasured, and found to be  $(2.9 \pm 0.2) \times 10^{-12} \text{ cm}^3 \text{ molecule}^{-1} \text{ s}^{-1}$  at  $299 \pm 1 \text{ K}$  at pressures of a few torr. These results are a clear indication that the observed kinetics of free radical reactions with hydrogen halides<sup>4,21,22</sup> in the gas phase are not affected by the reactions of any vibrationally excited states of the radical. The photogenerated free radicals are indeed collisionally deactivated in less than 0.5 ms by the buffer gas at the experimental conditions used. Thus an attempt to explain the kinetics measured in flow reactors<sup>22</sup> simply by heterogeneous wall reactions (caused by inadequate collisional relaxation of the radical with the buffer gas) is unreasonable and misleading.<sup>23</sup>

### Threshold energies

The kinetics of the CH<sub>2</sub>I + HBr reaction is shown in Fig. 2. The product of reaction (1) was detected to be CH<sub>3</sub>I. The transition states of the two reaction channels of the reverse reaction direction were characterized. In general, the energy barrier for abstracting a H atom by the Br atom on CH<sub>3</sub>I, CH<sub>2</sub>I<sub>2</sub> or CHI<sub>3</sub> is about 8–10 kJ mol<sup>-1</sup> larger than the competing channel for abstracting an I atom. This implies for instance that the reverse reaction (-1) cannot be studied experimentally. Solid evidence for this is provided in a crossed-molecular-beam experiment of the reaction Br + CH<sub>3</sub>I. The product IBr was concluded to be formed as the product of the reaction.<sup>24</sup>

The zero-point energy corrected threshold energy of reaction (-1) was determined by *ab initio* calculations at the MP2(fc)/6-311G(df)//MP2(fc)/6-311G(df) level of theory to be  $62.0 \text{ kJ mol}^{-1}$  at 0 K. More accurate calculations at the MP4(SDTQ)/6-311G(df)//MP2(fc)/6-311G(df) level yielded a similar value. On the other hand, the 3-21G basis set (the largest basis set available for iodine in Gaussian 98) is inadequate to calculate the threshold energy of reaction (-1) accurately. The other two quantum chemically calculated threshold energies for abstracting H atom at 0 K are  $48.0 \text{ kJ mol}^{-1}$  for Br + CH<sub>2</sub>I<sub>2</sub> and  $29.9 \text{ kJ mol}^{-1}$  for Br + CHI<sub>3</sub>. The threshold energies of the Br + molecule → HBr + radical reactions studied will be increased by  $1 \text{ kJ mol}^{-1}$  if the calculated zero-point energies are multiplied by 0.95 for the energy calculations. However, the scaling factor for unharmonic corrections is not used in the current study because no accurate value is known for it.

### Enthalpy of formation values determined

The enthalpy of formation of the CH<sub>2</sub>I radical was found to be  $228.0 \pm 2.8 \text{ kJ mol}^{-1}$  at 298 K. This value is in very good agreement with the value of  $228.4 \pm 8.4 \text{ kJ mol}^{-1}$  from the appearance energy measurement of Holmes and Lossing.<sup>25</sup> Furuyama *et al.* have used an iodination technique to determine the enthalpy of formation of CH<sub>2</sub>I to be  $230 \pm 7 \text{ kJ mol}^{-1}$ .<sup>26</sup> However, they assumed that the kinetics of the CH<sub>2</sub>I + I<sub>2</sub> reaction has no temperature dependence. More recent experiments on the free radical reactions with HBr and Br<sub>2</sub> indicate that the activation energy could be 2–3 kJ mol<sup>-1</sup> negative.<sup>21,27</sup> This would raise the enthalpy of formation value determined by Furuyama *et al.* to 232–233 kJ mol<sup>-1</sup>.

DeCorpo *et al.* determined  $\Delta_f H_{298}^0$  of the CH<sub>2</sub>I radical to be  $219.2 \pm 10 \text{ kJ mol}^{-1}$ .<sup>28</sup> The value was obtained from an appearance potential measurement of diiodomethane. However, a more recent  $\Delta_f H_{298}^0$  value<sup>19</sup> for CH<sub>2</sub>I<sub>2</sub> if used in their calculations would raise the enthalpy of formation of CH<sub>2</sub>I to  $225.4 \pm 10 \text{ kJ mol}^{-1}$  at 298 K.

The enthalpy of the CHI<sub>2</sub> radical was determined to be  $314.4 \pm 3.3 \text{ kJ mol}^{-1}$  at 298 K. According to this the C–H bond strength of the CH<sub>2</sub>I<sub>2</sub> molecule has a value of  $412.9 \pm 3.3 \text{ kJ mol}^{-1}$ . This value is clearly below the value of  $430 \pm 11 \text{ kJ mol}^{-1}$  determined in the studies of the reaction of CH<sub>2</sub>I<sub>2</sub> + HI ⇌ CH<sub>3</sub>I + I<sub>2</sub> using an iodination technique.<sup>29</sup> However,

this method includes inaccurately estimated activation energies for free radical reactions as mentioned above, a factor which typically leads to the calculated C–H bond energy being too large.<sup>30</sup> Moreover, it seems to be unrealistic to expect that the C–H bond energy of CH<sub>3</sub>I and CH<sub>2</sub>I<sub>2</sub> will be similar.<sup>29</sup> The threshold energy calculation is strong evidence that different energy barriers for the Br atom abstracting H atom from CH<sub>3</sub>I or CH<sub>2</sub>I<sub>2</sub> do exist. A similar trend of energy barriers as found in the current study is obtained for the other Br atom abstracting reactions with halogenated methanes.<sup>4</sup>

The  $\Delta_f H^\circ_{298}(\text{Cl}_3)$  was found to be  $424.9 \pm 2.8 \text{ kJ mol}^{-1}$ . This seems to be the first enthalpy of formation determination for the Cl<sub>3</sub> radical.

## Summary

The kinetics of the CH<sub>2</sub>I radical reaction with HBr has been characterized. The temperature dependence measured was combined with the *ab initio* calculated threshold energy of the reverse reaction to obtain the enthalpy of formation of CH<sub>2</sub>I radical to be  $228.0 \pm 2.8 \text{ kJ mol}^{-1}$  at 298 K. The C–H bond strength of iodomethane was calculated to be  $431.6 \pm 2.8 \text{ kJ mol}^{-1}$ . The trend of empirically determined activation energies of the forward free radical + HBr reactions was used with the *ab initio* calculated threshold energies of the reverse reactions to obtain  $\Delta_f H^\circ_{298}$  value for CHI<sub>2</sub> to be  $314.4 \pm 3.3 \text{ kJ mol}^{-1}$  and for Cl<sub>3</sub> to be  $424.9 \pm 2.8 \text{ kJ mol}^{-1}$ .

## Acknowledgements

This research was supported by the University of Helsinki, the Center for Scientific Computing at Espoo (both in Finland) and the National Science Foundation, Chemistry Division (USA). I also wish to thank Prof. Irene R. Slagle for kindly lending me the experimental apparatus for this study. The kinetic experiments were carried out at the Catholic University of America (Washington DC, USA).

## References

- J. E. Lovelock, R. J. Maggs and R. J. Wade, *Nature*, 1973, **241**, 194.
- R. M. Moore, R. Tokarczyk, V. K. Tait, M. Poulin and C. Green, *Naturally-Produced Organohalogens*, ed. A. Grimwall and E. de Leer, Kluwer, Dordrecht, 1995, p. 283.
- A. Jordan, J. Harnisch, R. Borchers, F. le Guern and H. Shinohara, *Environ. Sci. Technol.*, 2000, **34**, 1122.
- J. A. Seetula, *J. Chem. Soc., Faraday Trans.*, 1996, **92**, 3069.
- J. A. Seetula, *Phys. Chem. Chem. Phys.*, 2000, **2**, 3807.
- I. R. Slagle and D. Gutman, *J. Am. Chem. Soc.*, 1985, **107**, 5342.
- J. A. Seetula, *Ann. Acad. Sci. Fenn., Ser. A2*, 1991, 234.
- B. J. Huebert and R. M. Martin, *J. Phys. Chem.*, 1968, **72**, 3046.
- S. L. Baughcum and S. R. Leone, *J. Chem. Phys.*, 1980, **72**, 6531.
- J. Zhang and D. G. Imre, *J. Chem. Phys.*, 1988, **89**, 309.
- M. J. Frisch, G. W. Trucks, H. B. Schlegel, G. E. Scuseria, M. A. Robb, J. R. Cheeseman, V. G. Zakrzewski, J. A. Montgomery, Jr., R. E. Stratmann, J. C. Burant, S. Dapprich, J. M. Millam, A. D. Daniels, K. N. Kudin, M. C. Strain, O. Farkas, J. Tomasi, V. Barone, M. Cossi, R. Cammi, B. Mennucci, C. Pomelli, C. Adamo, S. Clifford, J. Ochterski, G. A. Petersson, P. Y. Ayala, Q. Cui, K. Morokuma, D. K. Malick, A. D. Rabuck, K. Raghavachari, J. B. Foresman, J. Cioslowski, J. V. Ortiz, B. B. Stefanov, G. Liu, A. Liashenko, P. Piskorz, I. Komaromi, R. Gomperts, R. L. Martin, D. J. Fox, T. Keith, M. A. Al-Laham, C. Y. Peng, A. Nanayakkara, C. Gonzalez, M. Challacombe, P. M. W. Gill, B. Johnson, W. Chen, M. W. Wong, J. L. Andres, C. Gonzalez, M. Head-Gordon, E. S. Replogle and J. A. Pople, *Gaussian 98, Revision A.3*, Gaussian, Inc., Pittsburgh, PA, 1998.
- J. B. Foresman and E. E. Frisch, *Exploring Chemistry with Electronic Structure Methods*, Gaussian, Inc., Pittsburgh, 2nd edn., 1996.
- M. P. McGrath and L. Radom, *J. Chem. Phys.*, 1991, **94**, 511.
- M. N. Glukhovtsev, A. Pross, M. P. McGrath and L. Radom, *J. Chem. Phys.*, 1995, **103**, 1878.
- J. A. Seetula, *J. Chem. Soc., Faraday Trans.*, 1998, **94**, 3561.
- P. J. Robinson, *J. Chem. Educ.*, 1978, **55**, 509.
- L. Pauling, *Nature of the Chemical Bond*, Cornell University Press, Ithaca, New York, 3rd edn., 1960.
- M. W. Chase, Jr., C. A. Davies, J. R. Downey, Jr., D. J. Frurip, R. A. McDonald and A. N. Syverud, *J. Phys. Chem. Ref. Data*, 1985, **14**, Supplement No. 1.
- A. S. Carson, P. G. Laye, J. B. Pedley and A. M. Welsby, *J. Chem. Thermodyn.*, 1993, **25**, 261.
- L. N. Krasnoperov and K. Mehta, *J. Phys. Chem. A*, 1999, **103**, 8008.
- J. A. Seetula and I. R. Slagle, *J. Chem. Soc., Faraday Trans.*, 1997, **93**, 1709.
- J. A. Seetula, J. J. Russell and D. Gutman, *J. Am. Chem. Soc.*, 1990, **112**, 1347.
- O. Dobis and S. W. Benson, *J. Am. Chem. Soc.*, 1995, **117**, 8171.
- The effects of reagent translational and vibrational energy on the dynamics of endothermic reactions*, D. Krajnovich, Z. Zhang, F. Huisken, Y. R. Shen and Y. T. Lee, *Phys. Electron. At. Collisions*, Invited Pap. Int. Conf., 12th, 1981, p. 733, ed. S. Datz, North-Holland Publishing Company, 1982, CAS 98:60192X.
- J. L. Holmes and F. P. Lossing, *Int. J. Mass Spectrom. Ion Processes*, 1984, **58**, 113.
- S. Furuyama, D. M. Golden and S. W. Benson, *Int. J. Chem. Kinet.*, 1969, **1**, 283.
- R. S. Timonen, J. A. Seetula, J. Niiranen and D. Gutman, *J. Phys. Chem.*, 1991, **95**, 4009.
- J. J. DeCorpo, D. A. Bafus and J. L. Franklin, *J. Chem. Thermodyn.*, 1971, **3**, 125.
- S. Furuyama, D. M. Golden and S. W. Benson, *J. Am. Chem. Soc.*, 1969, **91**, 7564.
- J. A. Seetula and D. Gutman, *J. Phys. Chem.*, 1991, **95**, 3626.